

# Non equilibrium steady states as resources for quantum heat engines

Francesco Tacchino,<sup>1,\*</sup> Tiago F. F. Santos,<sup>2</sup> Dario Gerace,<sup>1</sup> Michele Campisi,<sup>3,4,5</sup> and Marcelo F. Santos<sup>2,†</sup>

<sup>1</sup>*Dipartimento di Fisica, Università di Pavia, via Bassi 6, I-27100, Pavia, Italy*

<sup>2</sup>*Instituto de Física, Universidade Federal do Rio de Janeiro, CP68528, Rio de Janeiro 21941-972, Brazil*

<sup>3</sup>*NEST, Istituto Nanoscienze-CNR and Scuola Normale Superiore P.zza San Silvestro 12, I-56127 Pisa, Italy*

<sup>4</sup>*Dipartimento di Fisica e Astronomia, Università di Firenze, via Sansone 1, I-50019, Sesto Fiorentino (FI), Italy*

<sup>5</sup>*INFN Sezione di Firenze, via Sansone 1, I-50019, Sesto Fiorentino (FI), Italy*

(Dated: December 22, 2024)

When a quantum system is subject to a thermal gradient it may sustain a steady non-equilibrium heat current, by entering into a so-called non equilibrium steady state (NESS). Here we show that NESS constitute a thermodynamic resource that can be exploited to fuel a quantum heat engine. This adds to the list of recently reported sources available at the nano-scale, such as coherence, entanglement and quantum measurements. We elucidate this concept by showing analytic and numerical studies of a two-qubits quantum battery that is alternatively charged by a thermal gradient and discharged by application of a properly chosen unitary gate. The presence of a NESS for the charging step guarantees steady operation with positive power output. Decreasing the duration of the charging step results in a time periodic steady state accompanied by increased efficiency and output power. The device is amenable to implementation with different nanotechnology platforms.

## I. INTRODUCTION

With the fast advancement of nanotechnology, understanding and mastering the microscopic mechanisms that govern energy exchanges in nanoscale systems and devices has entered in the limelight of current research. This has led to a flourishing research activity aimed at singling out novel approaches to implement nano-thermal machines that take advantage of peculiar resources, e.g., of quantum nature, which are typically available only at minute scales and low-temperatures. It has already been pointed out that quantum coherences represent a genuinely quantum resource to be employed for fueling heat engines [1, 2]. A nano-heat engine operating thanks to a purely quantum effect (the AC Josephson effect) has been recently proposed [3], while it is expected that entanglement may, under special circumstances, constitute a thermodynamic resource as well [4–7]. Recently, another genuinely quantum effect, namely the invasive nature of the quantum measurement process, has been shown to also constitute a fuel for quantum heat engines [8]. Other works have focused on further aspects such as back-flow of information from the heat reservoirs [9], feedback control [10–12], and non-thermal-equilibrium dynamics [13], among others (for a recent review, see Ref. 14).

In this work, we single out yet another quantum property as a thermodynamic resource for quantum heat engines, namely the non-equilibrium steady state (NESS) that develops when a few level quantum system is in contact with two heat reservoirs at different temperatures, and is accordingly traversed by an incoherent heat flow.

A quantum thermal machine can be realized as a two-stroke engine, schematically shown in Fig. 1. In one stage the NESS develops in time, thus leading the quantum system to an *active* state, namely a state from which one can extract energy by means of a unitary operation. One can see this stage as the charging of a quantum battery. Here, the charging is caused by the application of a thermal gradient, while for common batteries it would be driven by the application of an electrochemical potential gradient. In the second stage, a unitary operation allows to extract the highest possible amount of energy stored in the quantum state of the system (i.e., the so called *ergotropy* [15]). The quantum battery is now in its *passive* state associated to the NESS, ready to be recharged and then start the cycle again.

We propose an implementation of the device with

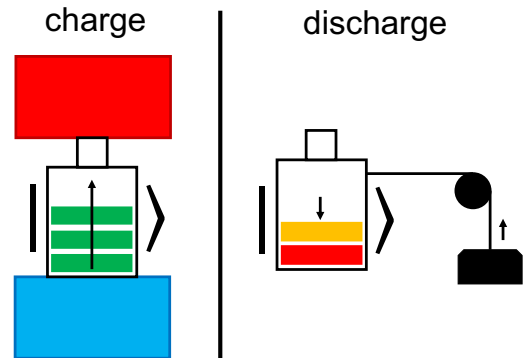


FIG. 1. Two stroke NESS-based quantum heat engine scheme: first the quantum working fluid playing the role of a quantum battery is charged, as it is traversed by an incoherent heat flux, and reaches a steady state; then, energy is extracted in the form of work by suitably coupling the battery to a work source that evolves it unitarily.

\* Present address: IBM Research GmbH, Zurich Research Laboratory, Säumerstrasse 4, CH-8803 Rüschlikon, Switzerland

† mfsantos@if.ufrj.br

state-of-art quantum optics technology, the working system being two coupled qubits. Numerical analysis validates the working principle and gives quantitative estimates for the expected efficiency and power output, respectively. We further analyse the thermodynamic performance as a function of the duration of the charging stroke. Remarkably, we show that for short charging times the quantum engine enters into a time periodic Floquet-type NESS after a few cycles, which is accompanied by enhanced output power and efficiency.

## II. THEORETICAL BACKGROUND

In the following we shall adopt the units convention where  $k_B = 1, \hbar = 1$ .

During the charging stroke the quantum system evolves while in contact with two heat baths at different temperatures. We shall model its dynamics via a Lindblad master equation

$$\dot{\rho} = \tilde{\mathcal{L}}(\rho) = -i[H, \rho] + \mathcal{L}(\rho). \quad (1)$$

The Lindblad superoperator,  $\tilde{\mathcal{L}}$ , contains a unitary part, stemming from the free evolution of the system dictated by its Hamiltonian,  $H$ , and a dissipative part,  $\mathcal{L} = \sum_j L_j$ , accounting for the coupling to the baths. Here the Lindblad operators  $L_j$  are of the form  $L_j(\rho) = \Gamma_j[J_j \rho J_j^\dagger - \frac{1}{2}\{J_j^\dagger J_j, \rho\}]$ , where  $\{A, B\} = AB + BA$ ,  $J_j$  are jump operators, and  $\Gamma_j$  are the related jump rates [16]. Formally, the solution of Eq. (1) reads

$$\rho(\tau) = e^{\tilde{\mathcal{L}}\tau} \rho = \sum_k M_k(\tau) \rho M_k(\tau)^\dagger \quad (2)$$

where the Kraus operators,  $M_k(\tau)$ , obey the relation  $\sum_k M_k^\dagger(\tau) M_k(\tau) = 1$ , depend on the duration  $\tau$  of the charging stroke, on the bath temperatures, and on the details of the couplings to the baths. We assume that the Lindblad operator has a fixed point,  $\rho_{NESS}$ , representing a non-equilibrium steady state,  $\tilde{\mathcal{L}}(\rho_{NESS}) = 0$ , which the system approaches for times longer than a characteristic time scale,  $\tau_{NESS}$ .

In the discharging stage a unitary operation,  $U_{\rho(\tau)}$ , is applied on the quantum system by means of the switching on of a properly designed coupling with an external work source (e.g., an electromagnetic field). The underlying assumption here is that the duration of this operation,  $\tau_d$ , is such that  $\tau_d \ll \tau$ . We shall accordingly treat this step as instantaneous, hence  $\tau$  will denote the duration of a complete cycle. Given the state  $\rho(\tau)$  at the beginning of the discharging stage, among all possible unitary operations, we obviously choose the one that extracts the maximal amount of energy. As shown in Ref. 15, such operation reads

$$\mathcal{E}_{\rho(\tau)} = \sum_{k,j} r_k E_j (|\langle r_k | E_j \rangle|^2 - \delta_{kj}) \quad (3)$$

where  $E_j$  are the eigenenergies of system Hamiltonian  $H$  ordered in increasing magnitude, i.e.,  $E_i \geq E_j$  for  $i > j$ , and  $r_k$  are the eigenvalues of the density operator  $\rho(\tau)$  in decreasing order, i.e.,  $r_i \leq r_j$  for  $i > j$ . Denoting their respective eigenvectors as  $|E_j\rangle$  and  $|r_j\rangle$ , the related unitary operation reads  $U_{\rho(\tau)} = \sum |E_j\rangle\langle r_j|$ , where we explicitly denoted its dependence on  $\rho(\tau)$ . The quantity  $\mathcal{E}_{\rho(\tau)}$  is known as the ergotropy of state  $\rho(\tau)$  [15]. Note that when  $\rho(\tau)$  and  $H$  commute, the unitary operation amounts to a permutation of the occupation probabilities of each energy eigenstate. The application of the unitary  $U_{\rho(\tau)}$  leaves the system in a so called passive state: a state from which one cannot extract any energy by means of unitary operations. In order for our engine to output work in a steady manner, it is crucial that the state at the beginning of each discharging stage be active, namely we need that the interaction with the baths activate the quantum system. In this respect, it is worth stressing that interaction with a single bath cannot fulfill this condition since thermalisation leads to the passive Gibbs state: in order to activate a system by means of thermal interactions, two baths are required at least.

Overall the (completely positive and trace preserving) map that advances the density operator of the working substance by one cycle reads:

$$\rho \rightarrow \sum_k U_{\rho(\tau)} M_k(\tau) \rho M_k^\dagger(\tau) U_{\rho(\tau)}^\dagger, \quad (4)$$

For the engine to be able to work cyclically it is necessary that the map above has a fixed point, which we shall refer to as the operational steady state  $\rho_{OSS}$ . In that case, as we shall see in our proposed implementation below, after a sufficient number of cycles (which may vary depending on  $\tau$ ) the system enters into a time-periodic Floquet-type steady state with period  $\tau$ . In that situation the energy gained during the charging stage balances with that given away during the discharging stage. In other words, at steady operation, the first stage pumps heat into the machine and takes the system from passive state  $\rho_{OSS}$  to its active counterpart  $\rho_{OSS}(\tau)$ , whereas the second stage extracts energy from the machine in the form of work and resets the system back to  $\rho_{OSS}$ .

Once the operational steady state is achieved, the power delivered reads  $P = \mathcal{E}_{\rho_{OSS}(\tau)}/\tau$ . The heat absorbed from the hot bath in a cycle reads [17]

$$Q^H(\tau) = \int_0^\tau dt \text{Tr} [L_H(\rho_{OSS}(t))H], \quad (5)$$

where  $L_H$  is the superoperator accounting for the effect of the coupling to the hot thermal source. The thermodynamic efficiency then reads  $\eta = \mathcal{E}_{\rho_{OSS}(\tau)}/Q^H(\tau)$ .

## III. TWO COUPLED QUBITS AS THE WORKING FLUID

From now on, we consider that the working fluid consists of two degenerate and mutually coupled qubits, with

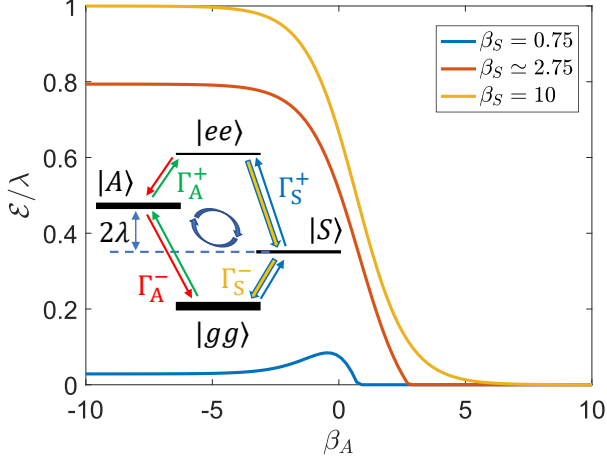


FIG. 2. Steady state ergotropy of the two coupled qubits setup as a function of inverse effective temperatures.  $\beta_S \simeq 2.75$  is equivalent to  $\Gamma_S^+ = \Gamma_A^+ = 3.5 \cdot 10^{-4} \omega_0$ ,  $\Gamma_S^- = 5.5 \cdot 10^{-3} \omega_0$  and  $\Gamma_A^- = 5 \cdot 10^{-4} \omega_0$ . These values were used in other simulations reported below. The inset shows the configuration of the energy levels with the transitions induced by external pumping and dissipation channels. The thickness of the levels represents the typical population distribution required to operate the thermal engine via the  $|A\rangle \leftrightarrow |S\rangle$  exchange.

energy gap  $\omega_0$  and coupling strength  $\lambda \ll \omega_0$ , schematically represented in Fig. 2a. The Hamiltonian reads

$$H = \omega_0(\sigma_+^{(1)}\sigma_-^{(1)} + \sigma_+^{(2)}\sigma_-^{(2)}) - \lambda(\sigma_+^{(1)}\sigma_-^{(2)} + h.c.) \quad (6)$$

where  $2\sigma_{\pm} = \sigma_x \pm i\sigma_y$  and  $\{\sigma_j\}$  for  $j = x, y, z$  are the Pauli matrices. The resulting energy levels, which can be obtained by direct diagonalization of  $H$ , are shown in the inset of Fig. 2 and correspond to the following set of total spin eigenstates

$$\begin{cases} |gg\rangle & E_{gg} = 0 \\ |S\rangle = \frac{1}{\sqrt{2}}(|ge\rangle + |eg\rangle) & E_S = \omega_0 - \lambda \\ |A\rangle = \frac{1}{\sqrt{2}}(|ge\rangle - |eg\rangle) & E_A = \omega_0 + \lambda \\ |ee\rangle & E_{ee} = 2\omega_0 \end{cases} \quad (7)$$

Here  $|g\rangle$  ( $|e\rangle$ ) denotes a qubit in the ground (excited) state. The two qubits are also coupled to two baths at temperatures  $\mathcal{T}_S$  and  $\mathcal{T}_A$ , each acting respectively on the symmetric (S) and anti-symmetric (A) transitions of the system, as depicted in Fig. 2. The overall dynamics of the machine will then follow Eq. (1) with  $\mathcal{L} = L_A + L_S$  where

$$\begin{aligned} L_A(\rho) &= \Gamma_A^+[A^\dagger \rho A - \frac{1}{2}\{AA^\dagger, \rho\}] + \Gamma_A^-[A \rho A^\dagger - \frac{1}{2}\{A^\dagger A, \rho\}], \\ L_S(\rho) &= \Gamma_S^+[S^\dagger \rho S - \frac{1}{2}\{SS^\dagger, \rho\}] + \Gamma_S^-[S \rho S^\dagger - \frac{1}{2}\{S^\dagger S, \rho\}] \end{aligned} \quad (8)$$

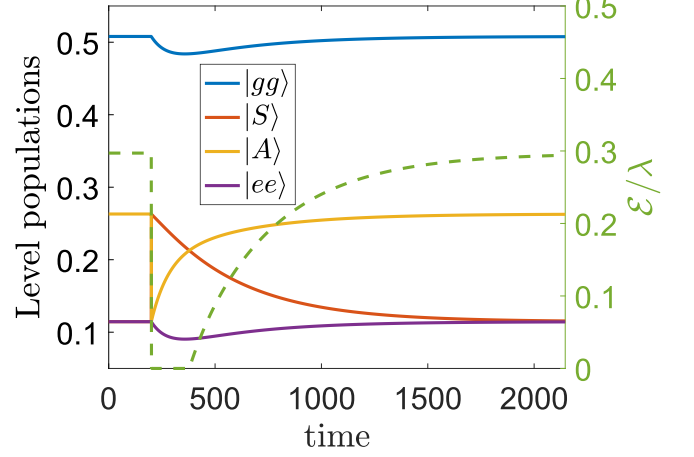


FIG. 3. Full cycle for the two-qubit thermal machine with instantaneous work extraction happening after a short idle phase and complete recharging to the NESS, shown in terms of the level populations as a function of time. Here parameters are chosen as  $\lambda = 10^{-2} \omega_0$ ,  $\Gamma_k^+ = \Gamma_0 \bar{n}_k$ ,  $\Gamma_k^- = \Gamma_0 (\bar{n}_k + 1)$ , with  $\bar{n}_k = 1/(e^{\omega_0/T_k} - 1)$ ,  $\mathcal{T}_A = 2\omega_0$ ,  $\mathcal{T}_S = 0.1\omega_0$  and  $\Gamma_0 = 10^{-3} \omega_0$ .

The rates  $\Gamma_{A,S}^\pm$  are given by

$$\Gamma_{A,S}^+ = \Gamma_{A,S}^0 \frac{1}{e^{\omega_0/\mathcal{T}_{A,S}} - 1} \quad \text{and} \quad \Gamma_{A,S}^- = \Gamma_{A,S}^0 \frac{e^{\omega_0/\mathcal{T}_{A,S}}}{e^{\omega_0/\mathcal{T}_{A,S}} - 1}, \quad (9)$$

where  $S^\dagger = \sigma_+^{(1)} + \sigma_+^{(2)}$  and  $A^\dagger = \sigma_+^{(1)} - \sigma_+^{(2)}$ . Note that these expressions are valid as long as  $\lambda \ll \omega_0$ . A possible quantum optical scheme to produce such dynamics was introduced in Ref. 7 and will be discussed in more detail later.

The general expression for the heat flux from the hot source ( $\mathcal{T}_A$ ) is given by

$$\dot{Q}^A = 4\omega_0(\Gamma_A^+ r_A - \Gamma_A^- r_e) + (\omega_0 + \lambda) \dot{r}_A \quad (10)$$

which, in the limit of  $\tau \rightarrow \infty$  ( $\dot{r}_j = 0$ ) becomes

$$\dot{Q}^A = 4\omega_0 \frac{\Gamma_A^+ \Gamma_S^- - \Gamma_A^- \Gamma_S^+}{\Gamma_A^+ + \Gamma_S^+} r_{S_{NESS}}. \quad (11)$$

Note that, if  $\Gamma_S^0 = \Gamma_A^0$ ,  $\dot{Q}^A$  is positive as long as  $\frac{\bar{n}_A}{\bar{n}_A+1} > \frac{\bar{n}_S}{\bar{n}_S+1}$  (where  $\frac{\bar{n}_k}{\bar{n}_k+1} = e^{-E_k/T_k}$ ), i.e. as long as there is a positive gradient temperature from  $\mathcal{T}_A$  to  $\mathcal{T}_S$ . This heat flow unbalances the population of the intermediate levels of the system in favour of the anti-symmetric state  $|A\rangle$ . This creates the necessary condition for the battery to store ergotropy. Moreover, the cyclic operation of the machine goes through operational states that are diagonal in the energy eigenbasis of the coupled qubits, i.e. of the type  $\rho_{OSS} = \sum_j r_j |j\rangle\langle j|$ , where  $j = \{gg, S, A, ee\}$ . In fact, there is a minimum period,  $\tau_{min}$ , beyond which a population inversion between the states A and S occurs:

$$r_{gg} > r_A > r_S > r_{ee} \quad (12)$$

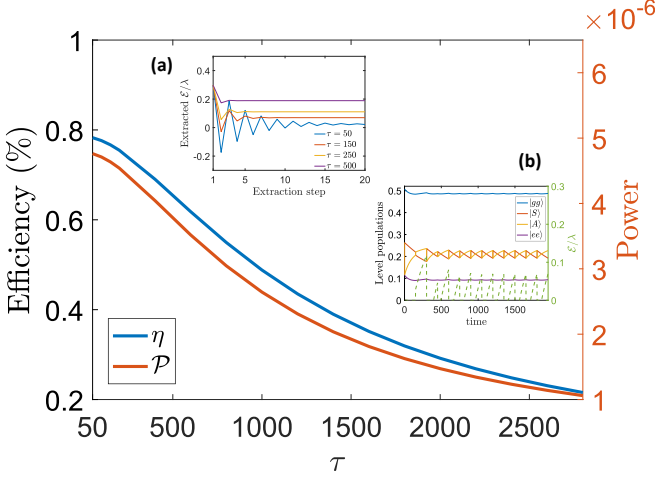


FIG. 4. Efficiency and power for the thermal machine operated at  $\rho_{OSS}$  as a function of  $\tau$ . Insets: (a) ergotropy extracted per step for different choices of  $\tau$  starting from  $\rho_{NESS}$  and converging to  $\rho_{OSS}$ ; (b) dynamics of the system reaching the operational steady state for  $\tau = 150$ . In all panels we set  $\lambda = 10^{-2}\omega_0$ ,  $\Gamma_k^+ = \Gamma_0\bar{n}_k$ ,  $\Gamma_k^- = \Gamma_0(\bar{n}_k + 1)$ , with  $\bar{n}_k = 1/(e^{\omega_0/T_k} - 1)$ ,  $\mathcal{T}_A = 2\omega_0$ ,  $\mathcal{T}_S = 0.1\omega_0$  and  $\Gamma_0 = 10^{-3}\omega_0$ .

accompanied by a non-zero ergotropy

$$\mathcal{E} = 2\lambda[r_A(\tau) - r_S(\tau)], \quad (13)$$

where  $\tau > \tau_{min}$ . Note that when  $\mathcal{T}_S = \mathcal{T}_A$ , then  $r_S = r_A$  and the ergotropy vanishes, making it clear that, indeed, a temperature gradient is crucial in order for the engine to work, as expected.

The machine here presented has some very distinctive properties. First of all, it is fuelled by a non-equilibrium steady state. Second, for the particular working fluid analysed,  $\rho_{OSS}$  is, in general, entangled [7] and there are three equally good unitary operations that maximize the extracted work: either a global operation  $U_{\mathcal{E}} = e^{-i(\sigma_z^{(1)} - \sigma_z^{(2)})\frac{\pi}{4}}$  or local ones  $U_{\mathcal{E}_i} = e^{-i\sigma_z^{(i)}\frac{\pi}{2}}$  where,  $i = \{1, 2\}$  indicates the qubit where  $U_{\mathcal{E}_i}$  is applied. That means that work can be fully extracted from one side or half of it simultaneously from both sides.

Third the efficiency of the machine depends on the chosen  $\rho_{OSS}$ . In Fig. 3, we show a full recharging stage as a function of time. At  $t = 0$  the system is in  $\rho_{NESS}$  when  $U_{\mathcal{E}}$  swaps the  $|A\rangle$  and  $|S\rangle$  populations. Then, the heat flowing from bath  $\mathcal{T}_A$  to  $\mathcal{T}_S$  recharges the battery. Note that even though larger periods allow for more stored energy in  $\rho_{OSS}$ , the most efficient operation takes place for shorter cycles. This is confirmed in Fig. 4 where we plot the efficiency and power as a function of the period of the cycle. Efficiency reaches a maximum plateau in the short cycle limit, when  $\sum_j \Gamma_j^\pm \tau \ll 1$ . In this case, up to first order in  $\tau$ , the ergotropy of  $\rho_{OSS}$  is given by

$$\mathcal{E}_\tau = 4\lambda\tau K(\Gamma_A^- + \Gamma_S^- - \Gamma_A^+ - \Gamma_S^+), \quad (14)$$

where  $K = (\Gamma_A^+\Gamma_S^- - \Gamma_A^-\Gamma_S^+)/(\Gamma_A^- + \Gamma_S^- + \Gamma_A^+ + \Gamma_S^+)^2$ , and

the incoming heat from the  $\mathcal{T}_A$  bath is given by

$$Q_\tau^A = 2K\tau [(\omega_0 - \lambda)(\Gamma_A^+ + \Gamma_S^+) + (\omega_0 + \lambda)(\Gamma_A^- + \Gamma_S^-)] \quad (15)$$

Therefore, the efficiency of the short cycle reads

$$\eta_\tau = \frac{2\lambda}{\omega_0} \frac{1 - \frac{\Gamma_A^+ + \Gamma_S^+}{\Gamma_A^- + \Gamma_S^-}}{1 + \frac{\lambda}{\omega_0} + \frac{\Gamma_A^+ + \Gamma_S^+}{\Gamma_A^- + \Gamma_S^-} (1 - \frac{\lambda}{\omega_0})} \quad (16)$$

For a fixed  $\lambda/\omega_0$  ratio,  $\eta_\tau$  is maximized when  $\Gamma_A^- + \Gamma_S^- \gg \Gamma_A^+ + \Gamma_S^+$ . This can be achieved either if both  $\mathcal{T}_A, \mathcal{T}_S \ll 1$  ( $\Gamma_j^- \gg \Gamma_j^+$ ) or if the cold reservoir ( $\mathcal{T}_S$  in our case) couples to the system in a much stronger way than the hot one ( $\Gamma_S^- \gg \Gamma_A^-$ ). In both scenarios,  $\eta_\tau \approx 2\lambda/(\omega_0 + \lambda)$ . The latter, however, is the one that produces the most power for the short cycle  $P_\tau = \mathcal{E}_\tau/\tau \approx 4\lambda\Gamma_A^+$ . Whereas the power for the first scenario depends on both temperatures and is given by  $P_\tau \approx 4\lambda(\Gamma_A^+\Gamma_S^- - \Gamma_A^-\Gamma_S^+)/(\Gamma_A^- + \Gamma_S^-)$ .

Finally, we show in the insets of Fig. 4 that a periodic Floquet-type NESS, here referred as  $\rho_{OSS}$ , is indeed reached for any choice of  $\tau$ . Inset (a) shows how many cycles are required to establish a steady operation for different periods, whereas inset (b) shows the stabilisation and the time evolution of the ergotropy of the machine for a particular choice of  $\tau$ .

Before concluding, let us remark that the main limitations to increase efficiency and power at short cycle operation are still the same ones for the model to hold true. On one hand,  $\tau \gg \tau_d$ , i.e. stage two must be much faster than stage one. On the other hand, the maximum efficiency and power require that  $\sum_j \Gamma_j^\pm \tau \ll 1$  (the short cycle regime). That ultimately limits  $\Gamma_A^+$ , and, thus, the generated power. How these limitations affect the operation of the machine will depend on the specificity of its physical implementation. That said, favorable conditions are already reachable in many practical setups as it is clear in quantum jumps experiments performed in different platforms [18–21].

We remark that the physical system described above can be implemented, as already discussed in a previous work [7], by two qubits that dissipate energy individually at rate  $\gamma$  and are incoherently pumped at rate  $p$ , while simultaneously coupled to a common superradiant bath that dissipates energy through the symmetric decay lines at rate  $\Gamma$ . In this case, as long as  $\lambda \ll \omega_0$ , the rates become  $\Gamma_S^+ = \Gamma_A^+ = p/2$ ,  $\Gamma_A^- = \gamma/2$  and  $\Gamma_S^- = \gamma/2 + \Gamma$  and the effective temperatures are given by  $\mathcal{T}_S = \frac{\omega_0}{\log(\frac{2\Gamma + \gamma}{p})}$  and  $\mathcal{T}_A = \frac{\omega_0}{\log(\frac{\gamma}{p})}$ . Maximum efficiency  $\eta_\tau = \frac{2\lambda}{\omega_0 + \lambda}$  is reached for  $\Gamma \gg \gamma, p$ , when the power becomes  $P_\tau \approx 2p\lambda$ .

#### IV. DISCUSSION

In summary, we have demonstrated that non-equilibrium steady states resulting from the application

of a thermal gradient onto a quantum system, constitute a thermodynamic resource. We have exemplified this statement by studying a model of two coupled qubits as the working fluid. We have shown that both efficiency and output power are maximized in the short cycle limit. We notice that the out-of-equilibrium quantum thermal machine discussed in this work can be realized in a variety of quantum technological platforms nowadays. On one hand, artificial atoms, such as semiconductor quantum dots [22] and superconducting quantum circuits [23], realize engineered coupled qubits and represent ideal, yet not fully explored playgrounds for quantum thermodynamics demonstrations. On an alternative ground, two trapped atoms or ions naturally represent a straightforward realization of quantum working fluids [24]. The former solid state platforms might be preferred due to the possibility of engineering the system parameters, such as energy gaps and coupling rates, where in natural systems these parameters of the model are fixed or with limited tunability, thus producing low efficiency and output power.

We remark that the presented concept is general and widely applicable. The quantum battery need not be a two-qubit system, on the contrary it can generally be a many-body quantum system comprising e.g., several qubits, or qutrits etc., harmonic or anharmonic oscil-

lators, coupled via short-range or long-range forces. Accordingly, the presented concept lends itself to a promising broader investigation regarding the possible positive impact of many-body phenomena, such as many-body entanglement, phase transitions, collective behaviour (e.g. superradiance) on the thermodynamic performance of NESS based engines. Note that previous works have already pointed out their positive impact on the standard charging of quantum batteries by external fields, see e.g., [4, 25], and on the performance of Otto engines [26]. Other meaningful follow up directions of the current work are related to the study of the impact of non-Markovian (instead of Lindblad-type) recharging first stages on both efficiency and generated power, as well as the effects of a non-ideal energy extracting second stage.

## V. ACKNOWLEDGEMENTS

MFS acknowledges FAPERJ Project No. E-26/202.576/2019 and CNPq Projects No. 302872/2019-1 and INCT-IQ 465469/2014-0. MFS would also like to thank the CICOPS program from the University of Pavia for hospitality and support. TFFS acknowledges CAPES for financial support.

- 
- [1] M. O. Scully, M. S. Zubairy, G.S. Agarwal and H. Walther, Extracting Work from a Single Heat Bath via Vanishing Quantum Coherence, *Science*, **299**, 862-864 (2003)
  - [2] J. Klatzow, J. N. Becker, P. M. Ledingham, C. Weinzetl, K. T. Kaczmarek, D. J. Saunders, J. Nunn, I. A. Walmsley, R. Uzdin and E. Poem, Experimental Demonstration of Quantum Effects in the Operation of Microscopic Heat Engines, *Phys. Rev. Lett.*, **122**, 110601 (2019)
  - [3] G. Marchegiani, P. Virtanen, F. Giazotto and M. Campisi, Self-Oscillating Josephson Quantum Heat Engine, *Phys. Rev. Applied*, **6**, 054014 (2016)
  - [4] F. Campaioli, F. A. Pollock, F. C. Binder, L. Céleri, J. Goold, S. Vinjanampathy, and K. Modi, Enhancing the Charging Power of Quantum Batteries, *Phys. Rev. Lett.*, **118**, 150601 (2017)
  - [5] G. Francica, J. Goold, F. Plastina and M. Paternostro, Daemonic ergotropy: enhanced work extraction from quantum correlations, *npj Quantum Information*, **3**, 12 (2017)
  - [6] F. Sapienza, F. Cerisola and A. J. Roncaglia, Correlations as a resource in quantum thermodynamics, *Nature Communications*, **10**, 2492 (2019)
  - [7] F. Tacchino, A. Auffèves, M. F. Santos and D. Gerace, Steady State Entanglement beyond Thermal Limits, *Phys. Rev. Lett.*, **120**, 063604 (2018)
  - [8] L. Buffoni, A. Solfanelli, P. Verrucchi, A. Cuccoli and M. Campisi, Quantum Measurement Cooling, *Phys. Rev. Lett.*, **122**, 070603 (2019)
  - [9] B. Bylicka, M. Tukiainen, D. Chruściński, J. Piilo and S. Maniscalco, Sabrina, Thermodynamic power of non-Markovianity, *Scientific Reports*, **6**, 27989 (2016)
  - [10] M. Campisi, J. Pekola and R. Fazio, Feedback-controlled heat transport in quantum devices: theory and solid-state experimental proposal, *New J. Phys.*, **19**, 053027 (2017)
  - [11] H. Quan, Y. Wang, Yu-xi Liu, C. Sun and F. Nori, Maxwell's Demon Assisted Thermodynamic Cycle in Superconducting Quantum Circuits, *Phys. Rev. Lett.*, **97**, 180402 (2006)
  - [12] S. Toyabe, T. Sagawa, M. Ueda, E. Muneyuki and M. Sano, Experimental demonstration of information-to-energy conversion and validation of the generalized Jarzynski equality, *Nature Physics*, **6**, 988–992 (2010)
  - [13] F. Barra, Dissipative Charging of a Quantum Battery, *Phys. Rev. Lett.*, **122**, 210601 (2019)
  - [14] R. Kosloff A. and Levy, Quantum Heat Engines and Refrigerators: Continuous Devices, *Annu. Rev. Phys. Chem.*, **65** (2014)
  - [15] A. E. Allahverdyan, R. Balian and Th. M. Nieuwenhuizen, Maximal work extraction from finite quantum systems, *EPL* **67**, 565–571 (2004)
  - [16] H. P. Breuer and F. Petruccione, *The theory of open quantum systems* (Oxford University Press, 2002)
  - [17] R. Alicki, The quantum open system as a model of the heat engine, *J. Phys. A: Math. Gen.*, **12** L103 (1979)
  - [18] C. Sayrin, I. Dotsenko, X. Zhou, B. Peaudecerf, T. Rybarczyk, S. Gleyzes, P. Rouchon, M. Mirrahimi, H. Amini, M. Brune, J-M. Raimond and S. Haroche, Real-time quantum feedback prepares and stabilizes photon number states, *Nature*, **477**, 73–77 (2011)
  - [19] Z. K. Mineev, S. O. Mundhada, S. Shankar, R. P. Reinhold, R. Gutiérrez-Jáuregui, R. J. Schoelkopf, M. Mirrahimi, H. J. Carmichael and M. H. Devoret, To catch

- and reverse a quantum jump mid-flight, *Nature*, **570**, 200–204 (2019)
- [20] S. Gleyzes, S. Kuhr, C. Guerlin, J. Bernu, S. Deléglise, U. Busk Hoff, M. Brune, J.-M. Raimond and S. Haroche, Quantum jumps of light recording the birth and death of a photon in a cavity, *Nature*, **446**, 297–300 (2007)
- [21] R. Vijay, D. H. Slichter and I. Siddiqi, Observation of Quantum Jumps in a Superconducting Artificial Atom, *Phys. Rev. Lett.*, **106**, 110502 (2011)
- [22] M. Josefsson, A. Svilans, A. M. Burke, E. A. Hoffmann, S. Fahlvik, C. Thelander, M. Leijnse and H. Linke, A quantum-dot heat engine operating close to the thermodynamic efficiency limits, *Nature Nanotechnology*, **13**, 920–924 (2018)
- [23] J. P. Pekola, Towards quantum thermodynamics in electronic circuits, *Nature Physics*, **11**, 118–123 (2015)
- [24] J. Roßnagel, S. T. Dawkins, K. N. Tolazzi, O. Abah, E. Lutz, F. Schmidt-Kaler and K. Singer, A single-atom heat engine, **352**, 325–329 (2016)
- [25] D. Ferraro, M. Campisi, G. M. Andolina, V. Pellegrini and M. Polini, High-Power Collective Charging of a Solid-State Quantum Battery, *Phys. Rev. Lett.*, **120**, 117702 (2018)
- [26] M. Campisi and R. Fazio, The power of a critical heat engine, *Nat Commun*, **7**, 11895 (2016)